

Frequency Upconversion in Er³⁺/Yb³⁺ Codoped Lead Bismuth Gallium Borate Glasses

K Krishna Murthy Goud^{1*}, Ch Ramesh² and B Appa Rao³

¹Dept. of Physics, UCE (A), Osmania University, Hyderabad-500007 (T.S), India.

²Dept. of Physics, M G University, Nalgonda (T.S), India.

³Dept. of Physics, Osmania University, Hyderabad-500007 (T.S), India.

Abstract

Lead bismuth gallium borate (GEY) glasses codoped with Er³⁺/Yb³⁺ were prepared by melt quenching technique. The glasses were characterized by X-ray diffraction spectra. Optical absorption, FTIR and photoluminescence spectra of these glasses have been studied. The optical absorption spectra exhibits a band at 980 nm due to transitions from the ground states ⁴I_{15/2} and ²F_{7/2} to excited states of Er³⁺ and Yb³⁺ respectively. The other absorption bands at 488nm, 521 nm, 545 nm, 652 nm, 798 nm and 1510 nm are attributed to transitions from the ground state ⁴I_{15/2} to excited state of Er³⁺. Judd-Ofelt theory has been applied to the f ↔ f transitions for evaluating Ω₂, Ω₄ and Ω₆ parameters. Radiative properties like branching ratio β_r and the radiative life time τ_R have been determined on the basis Judd-Ofelt theory. Upconversion emissions have been observed under 980nm laser excitation at room temperature. Green and red up-conversion emissions are centered at 525, 545 and 660 nm corresponding to ²H_{11/2} → ⁴I_{15/2}, ⁴S_{3/2} → ⁴I_{15/2} and ⁴F_{9/2} → ⁴I_{15/2} transitions of Er³⁺ respectively. The results obtained are discussed quantitatively based on the energy transfer between Yb³⁺ and Er³⁺.

Keywords: Optical absorption, FTIR, Photo luminescence

1. INTRODUCTION

Recently, there has been great interest in the conversion of infrared light to visible light through energy upconversion in rare-earth doped glasses, due to the possibility of infrared-pumped visible lasers and the potential applications in areas such as optical

data storage, lasers, sensors, and optical displays [1-3]. Among different oxide glass compositions, lead borate glasses doped with rare earth ions seems to be very attractive systems for applications in optical devices of laser technology. The absorption and emission properties of rare earth ions in lead borate glasses are well reported in the literature [4-6]. Among various glass systems, heavy metal oxide based glass systems find potential applications in non-linear optical devices because of their high refractive index and low phonon energy compared with other glasses [7].

Ga₂O₃ is a heavy metal oxide and when it is introduced in the glass matrix, is expected to alter the physical properties like refractive index, thermal expansion coefficient, chemical resistance and glass transition temperature, infrared transmittance and the insulating strength of the glasses spectacularly and makes the glasses suitable for the applications like in infrared windows, ultra-fast optical switches, optical isolators and other photonic devices [8, 9]. Among various rare-earth ions that emit upconversion fluorescence, Er³⁺ is the most widely studied as an active ion and gives rather high efficiency. In general, the most efficient are energy transfer upconversion and excited state absorption processes in the case of the Er³⁺ ion [10]. The sensitization of Er³⁺ doped materials with Yb³⁺ ions is a well-known method for increasing the optical pumping efficiency because of the efficient energy transfer from Yb³⁺ to Er³⁺ ions [11]. In this investigation, a series of Er³⁺/Yb³⁺ codoped lead bismuth gallium borate glasses have been prepared. The XRD, optical absorption, FTIR and upconversion fluorescence spectra have been measured for these samples and the results are discussed in detail.

2. EXPERIMENTAL

For the present study glasses with [100-(x+y)] [0.5PbO-0.25B₂O₃-0.20Bi₂O₃-0.05Ga₂O₃]-xEr₂O₃-yYb₂O₃ with y = 0 for x = 0, 0.2 and y = 0.2 for x = 0 to 1.0 (step 0.2 mol%) are chosen and the glass samples are labelled as GE0Y0, GE2Y0, GE0Y2, GE2Y2, GE4Y2, GE6Y2, GE8Y2 and GE10Y2 respectively. Appropriate amounts of AR grade reagents of PbO, B₂O₃, Bi₂O₃, Ga₂O₃, Er₂O₃ and Yb₂O₃ powders were weighed by using digital electronic balance. These chemicals were mixed and thoroughly ground in a mortar to get a homogeneous mixture and melted in a porcelain crucible in the temperature range of 900 to 950 °C in a programmable electrical furnace for thirty minutes until bubble free liquid is formed. The resultant melt is poured in a brass mould and subsequently annealed at 300 °C for about four hours in order to avoid these internal mechanical stresses.

The optical absorption spectra were obtained with the JASCO Model V-670 UV-VIS-NIR spectrophotometer in the wavelength range 350–2000 nm with a spectral resolution of 0.1 nm. The FTIR spectra of glass samples were recorded on a BRUKER OPTICS, TENSOR-27 infrared spectrometer in the range 4000 – 400 cm⁻¹. For IR measurements, the glasses were pulverized and mixed with KBr in order to obtain thin pellets with a thickness of about 0.3mm. The visible upconversion fluorescence spectra were recorded using JOBIN YVON Fluorolog-3 spectrofluorimeter in the wavelength range 300-700 nm under the excitation of 980 nm laser diode.

3. RESULTS AND DISCUSSION

3.1 Optical absorption

Figure 1 shows optical absorption spectra of all prepared glass samples. The spectra exhibits intense absorption band at 980 nm due to $^4\text{I}_{15/2} \rightarrow ^4\text{I}_{11/2}$ and $^2\text{F}_{7/2} \rightarrow ^2\text{F}_{5/2}$ transitions of Er^{3+} and Yb^{3+} , respectively. The other absorption bands are attributed to 4f-4f transitions of Er^{3+} ions from the ground ($^4\text{I}_{15/2}$) state to the excited states at 488 nm ($^4\text{F}_{7/2}$), 521 nm ($^2\text{H}_{11/2}$), 545 nm ($^4\text{S}_{3/2}$), 652 nm ($^4\text{F}_{9/2}$), 798 nm ($^4\text{I}_{9/2}$) and 1510 nm ($^4\text{I}_{13/2}$) [12, 23]. The intensities of all bands was found to increase with increase in the concentration of Er^{3+} ions. There is no significant shift is observed in the band positions.

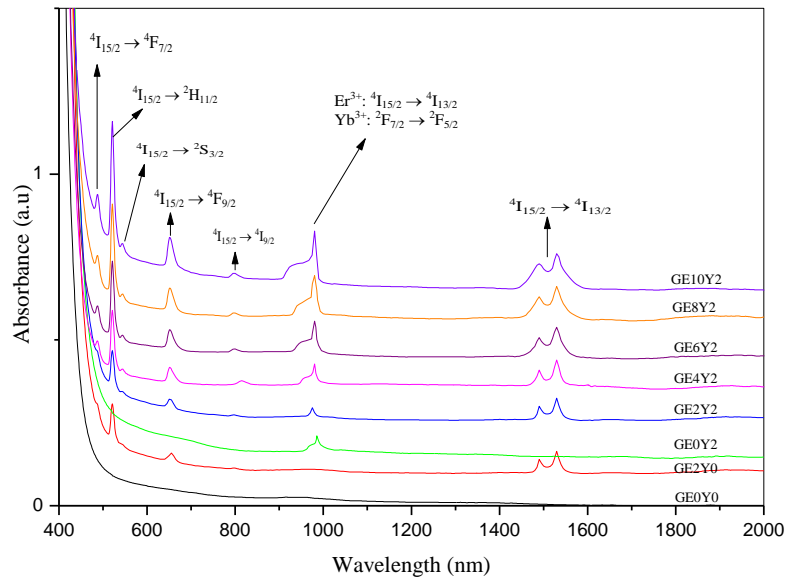


Figure 1. Optical absorption spectra of GEY glass system.

From the spectra it was observed that cut-off wavelength value increases upto 0.6 mol% (GE6Y2) of Er^{3+} ions and decreases further with increase in the concentration of Er^{3+} ions. Using standard relations the values of optical band gap and the Urbach energy are calculated [13, 14]. From the data (Table 1) the value of E_{opt} was found to decrease upto 0.6 mol% (GE6Y2) of Er^{3+} ions and increases further with increase in the concentration of Er^{3+} ions. The decrease in the optical band gap with the increase in the concentration of Er_2O_3 up to 0.6 mol% suggests increasing degree of depolymerization or concentration of bonding defects and non-bridging oxygens (NBO) in the glass network up to this concentration of Er_2O_3 . Probably in this concentration range the gallium ions may take network forming positions with GaO_4 structural units and alternate with BO_4 units. Such linkages may cause a decrease in the rigidity of the glass network and leads to the decrease in the optical band gap as observed. The Judd-Ofelt theory helps in the analyzation of the radiative transitions within in the $4f^N$ configuration of a rare earth ion. The Judd-Ofelt parameters Ω_2 , Ω_4 and Ω_6 [15, 16] can be determined by obtaining the experimental ground state oscillator strengths of the

absorption transitions via an integration of the absorption coefficients for each band. The Judd-Ofelt theory has often been used to calculate the spectroscopic parameters, such as radiative lifetime, oscillator strength and branching ratios (β_r) using standard equations [17-22]. The results are summarized in Table 2 and Table 3.

According to literature [23, 24], Ω_2 is related with the symmetry of the rare earth site while Ω_6 is inversely proportional to the covalency of Er-O bond. The Er-O bond is assumed to be dependent on the local basicity around the rare-earth (RE) sites, which can be adjusted by the composition or structure of the glass hosts. It is well established that an emission level with β_r value above 50% becomes a potential laser emission. Referring to the data on emission transitions in the present glass system, the transition ${}^4F_{9/2} \rightarrow {}^4I_{15/2}$ has the highest value of β_r among various transitions. This transition may therefore considered as a possible laser transition. The values of Judd-Ofelt parameters it was found to be in the order $\Omega_2 > \Omega_4 > \Omega_6$.

Table 1. Values of cut off wavelength, optical band gap and urbach energy GEY glass system doped with $\text{Er}^{3+}/\text{Yb}^{3+}$.

S.No.	Sample code	Cut-off wavelength (nm)	E_{opt} (eV) ± 0.01	ΔE (eV) ± 0.001
1	GE0Y0	400	3.02	0.152
2	GE2Y0	408	2.96	0.148
3	GE0Y2	409	2.95	0.148
4	GE2Y2	419	2.89	0.144
5	GE4Y2	425	2.85	0.139
6	GE6Y2	431	2.80	0.135
7	GE8Y2	427	2.83	0.138
8	GE10Y2	423	2.86	0.141

Table 2. Radiative life time (τ_R) and branching ratios (β_r) of Er^{3+} in GEY glass.

Transitions	β_r (%)	τ_R (ms)
${}^2H_{11/2} \rightarrow {}^4I_{15/2}$	14	0.74
${}^4S_{3/2} \rightarrow {}^4I_{15/2}$	16	0.80
${}^4F_{9/2} \rightarrow {}^4I_{15/2}$	52	2.76

3.2 FTIR

The FTIR spectra of GEY glass system codoped with Er^{3+}/Yb^{3+} was shown in figure 2. A band cited in the region $\sim 482\text{ cm}^{-1}$ is identified due to bending vibrations of Bi_2O_3 pyramidal units and also due to the presence of PbO_4 structural units [25]. A band cited in the region $\sim 613\text{ cm}^{-1}$ is identified due to network forming GaO_4 tetrahedral groups [26]. The band cited at $\sim 707\text{ cm}^{-1}$ and is attributed to the vibrations of B-O-B linkages. A band cited in the region $\sim 930\text{ cm}^{-1}$ is assigned to asymmetric stretching vibrations of B-O bands in BO_4 units. The band cited in the region $\sim 1250\text{ cm}^{-1}$ is identified due to asymmetric stretching modes of borate triangles BO_3 and BO_2O^- .

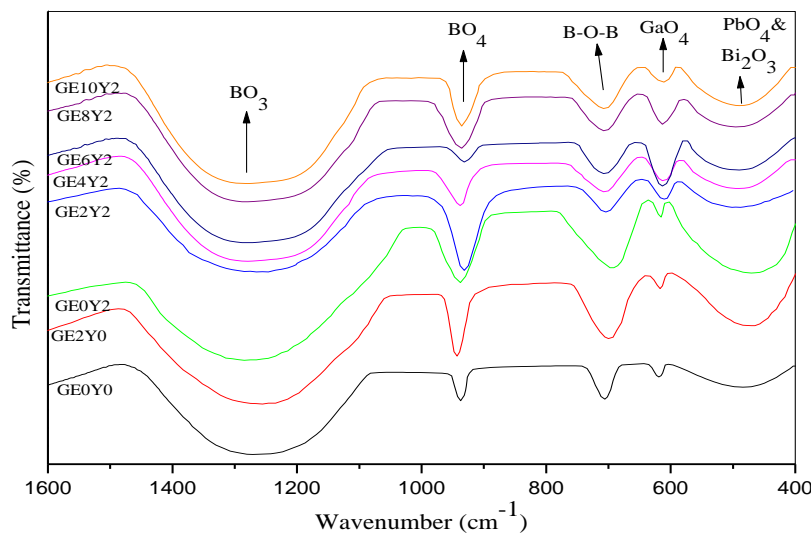


Figure 2. FTIR spectra of GEY glass system.

Ga_2O_3 is considered to act as a network former if Ga^{3+} ions take preferentially fourfold coordination in oxide glasses. The excess negative charge on GaO_4 tetrahedra is compensated either by localization of a modifier ion nearby or by generation of threefold oxygens. The GaO_4 tetrahedrons may enter the glass network and alternate with BO_4 tetrahedrons. In some of the glass networks, the gallium ions are also found to be in modifier positions with GaO_6 structural units [27]. From the spectra it was observed that intensity of band corresponding to GaO_4 tetrahedral groups increases from 0 mol% of Er^{3+} ions (GE0Y0) to 0.6 mol% of Er^{3+} ions (GE6Y2), beyond this concentration the trend is reverse. This is due to the fact that Ga^{3+} ions go into substitutional positions with GaO_4 structural units and alter the glass network upto 0.6 mol%. Within this concentration Ga^{3+} ions, isolate the rare-earth ions from RE-O-RE bonds and form Ga-O-RE bonds. Such declustering effect leads to the larger spacing between RE ions and may contributes for the enhancement of fluorescence emission.

3.3 UPCONVERSION

Figure 3 represents the upconversion emission spectra of Er^{3+}/Yb^{3+} codoped GEY glass system in the wavelength range of 500 –700 nm under the excitation of 980 nm laser

diode at room temperature. The spectra exhibited three emission bands centered at 525 nm ($^2H_{11/2} \rightarrow ^4I_{15/2}$), 545 nm ($^4S_{3/2} \rightarrow ^4I_{15/2}$) and 660 nm ($^4F_{9/2} \rightarrow ^4I_{15/2}$). It was observed that the upconversion luminescence intensity of red emission (660 nm) is higher than the upconversion luminescence intensity of green emission (525 and 545 nm). It is also important to point out that the green emission is very weak and red emission is very prominent to be observed by the naked eye at low excitation power for Er^{3+}/Yb^{3+} codoped GEY glass system at room temperature.

Table 3. Experimental and calculated oscillator strength of Er^{3+} in GEY glass.

Transition from $^4I_{15/2} \rightarrow$	$f_{exp}(x10^{-6})$	$f_{cal}(x10^{-6})$
$^4I_{13/2}$	0.982	0.976
$^4I_{11/2}$	0.549	0.558
$^4I_{9/2}$	0.446	0.441
$^4F_{9/2}$	1.207	1.219
$^4S_{3/2}$	0.328	0.312
$^2H_{11/2}$	4.435	4.442
$^4F_{7/2}$	1.163	1.171
r.m.s. deviation	± 0.091	

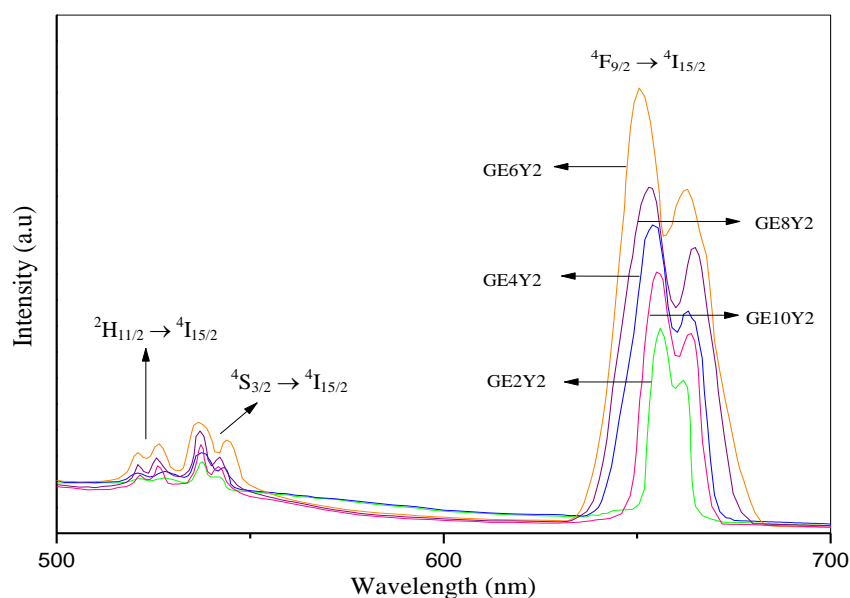


Figure 3. Frequency upconversion emission spectra of Er^{3+}/Yb^{3+} codoped glasses.

From the spectra it can be concluded that the intensity of green and red emissions increases with increase in the concentration of Er^{3+} ions upto 0.6 mol% (GE6Y2) and

decreases with further increase in the concentration of Er^{3+} ions in Er^{3+}/Yb^{3+} codoped glass samples. In an upconversion, the emission intensity (I_{up}) increases in proportion to the n^{th} power of infrared excitation intensity (I_{IR}), i.e.,

$$I_{up} \propto I_{IR}^n$$

where n is the number of IR photons absorbed per visible photon emitted [28]. A plot of $\log I_{up}$ versus $\log I_{IR}$ yields a straight line with slope 'n'. Figure 4 shows such a plot for the 660 nm emissions under 980 nm excitation. From figure 5 the slope value (n) for the 660 nm emission band was calculated and got around two. The results shows that a two photon upconversion process is responsible for the green (525, 545 nm) and red (660 nm) emissions from the ${}^2H_{11/2} \rightarrow {}^4I_{15/2}$, ${}^4S_{3/2} \rightarrow {}^4I_{15/2}$ and ${}^4F_{9/2} \rightarrow {}^4I_{15/2}$ transitions, respectively [29].

The possible upconversion mechanisms for the emissions in the Er^{3+}/Yb^{3+} codoped GEY glass system under 980 nm excitation are explained based on the energy matching conditions and the quadratic dependence on 980 nm pump intensity as illustrated in Fig. 5 [30]. The energy transfer mechanism for the green emissions as follows (Process-I) : in the first step, the ${}^4I_{11/2}$ level is directly excited with 980 nm light by ground state absorption (GSA) and/or by the energy transfer (ET) process from ${}^2F_{5/2}$ level of Yb^{3+} : ${}^2F_{5/2}(Yb^{3+}) + {}^4I_{15/2}(Er^{3+}) \rightarrow {}^4I_{11/2}(Er^{3+}) + {}^2F_{7/2}(Yb^{3+})$. Due to much larger absorption cross-section of Yb^{3+} than Er^{3+} in the 980 nm region, the energy transfer (ET) process is dominant to the excitation of ${}^4I_{11/2}$ level. The second step involves the excitation processes based on the long-lived ${}^4I_{11/2}$ level as follows: excited state absorption (ESA) ${}^4I_{11/2}(Er^{3+}) + \text{a photon} \rightarrow {}^4F_{7/2}(Er^{3+})$ and ET ${}^2F_{5/2}(Yb^{3+}) + {}^4I_{11/2}(Er^{3+}) \rightarrow {}^2F_{7/2}(Yb^{3+}) + {}^4F_{7/2}(Er^{3+})$. For an Er^{3+} ion in the ${}^4F_{7/2}$ excited state the interaction with a nearby Er^{3+} ion in the ground state would lead to two Er^{3+} ions at the ${}^4I_{11/2}$ level. This process can be represented as follows: ${}^4F_{7/2}(Er^{3+}) + {}^4I_{15/2}(Er^{3+}) \rightarrow {}^4I_{11/2}(Er^{3+}) + {}^4I_{11/2}(Er^{3+})$. However, the transition probability involved in the above processes can be small, and so the ${}^4F_{7/2}$ level is populated. The populated Er^{3+} ${}^4F_{7/2}$ level then relaxes rapidly and non-radiatively to the next lower levels, ${}^2H_{11/2}$ and ${}^4S_{3/2}$ resulting from the small energy gap between them. Er^{3+} ions at the ${}^2H_{11/2}$ level can also decay to the ${}^4S_{3/2}$ level due to multiphonon relaxation process. The estimated energy gap between the ${}^2H_{11/2}$ level and the next lower level ${}^4S_{3/2}$ is about 800 cm^{-1} . Thus, multiphonon relaxation rate is very large and the 525 nm emission intensity will be reduced [31]. Most of the erbium ions at ${}^4S_{3/2}$ level relaxes non-radiatively to the next lower level (${}^4F_{9/2}$). Hence the intensity of green emissions centered at 525 nm and 545 nm are very small as observed in the upconversion spectra. In this way the above mechanism is responsible for the green emissions centered at 525 and 545 nm corresponding to the ${}^2H_{11/2} \rightarrow {}^4I_{15/2}$ and ${}^4S_{3/2} \rightarrow {}^4I_{15/2}$ transitions, respectively.

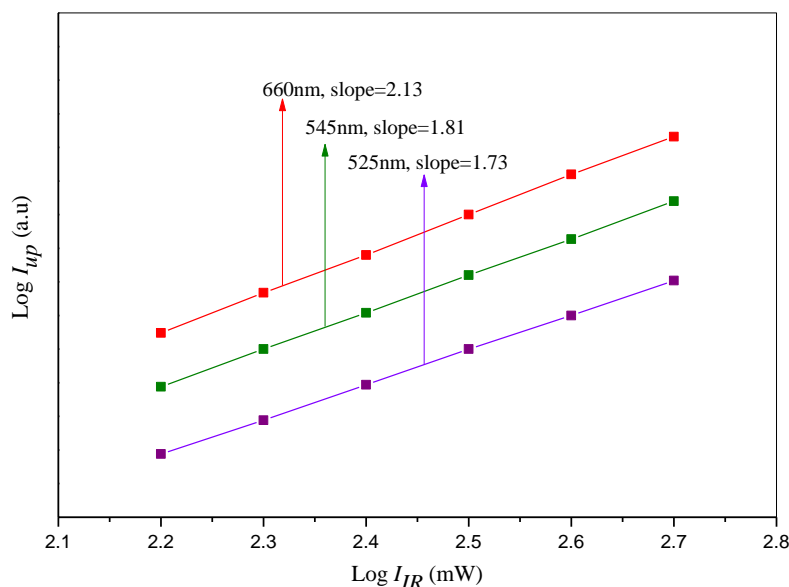


Figure 4. Dependence of upconversion fluorescence intensity on excitation power under 980 nm excitation

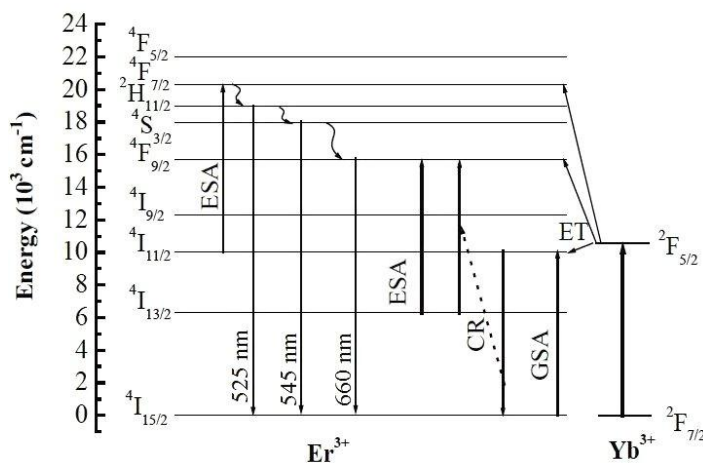


Figure 5. Energy level diagram of $\text{Er}^{3+}/\text{Yb}^{3+}$ codoped GEY glass system under the excitation of 980 nm laser diode [35].

The energy transfer mechanism for the red emission at 660 nm (${}^4\text{F}_{9/2} \rightarrow {}^4\text{I}_{15/2}$) as follows (Process-II): excited state absorption (ESA): ${}^4\text{I}_{13/2}(\text{Er}^{3+}) + \text{a photon} \rightarrow {}^4\text{F}_{9/2}(\text{Er}^{3+})$ and cross-relaxation (CR) between Er^{3+} ions: ${}^4\text{I}_{13/2}(\text{Er}^{3+}) + {}^4\text{I}_{11/2}(\text{Er}^{3+}) \rightarrow {}^4\text{I}_{15/2}(\text{Er}^{3+}) + {}^4\text{F}_{9/2}(\text{Er}^{3+})$, and ET from Yb^{3+} : ${}^2\text{F}_{5/2}(\text{Yb}^{3+}) + {}^4\text{I}_{13/2}(\text{Er}^{3+}) \rightarrow {}^2\text{F}_{7/2}(\text{Yb}^{3+}) + {}^4\text{F}_{9/2}(\text{Er}^{3+})$. The ${}^4\text{I}_{13/2}$ level is populated owing to the non-radiative relaxation from the upper ${}^4\text{I}_{11/2}$ level. Besides, the non-radiative process from ${}^4\text{S}_{3/2}$ level, which is populated by means of the process described previously, to the ${}^4\text{F}_{9/2}$ level also contributes to the red emission. The

experimental evidence of the enhancement of the red emission when compared to the green emission can be explained by the process-II. The number of Er^{3+} ions in the $^4\text{I}_{11/2}$ level relaxing non-radiatively to the lower $^4\text{I}_{13/2}$ level are much greater than those excited to the upper $^4\text{F}_{7/2}$ level via process-I. The much longer lifetime of $^4\text{I}_{13/2}$ state when compared with the lifetime of the $^4\text{I}_{11/2}$ state [32, 33] makes the process-II dominant over the process-I for the red emission. The green emission cannot be populated by the process-II. Moreover, as mentioned before, the phonon energy also plays an important role and it can affect the upconversion intensity: with the increase of the phonon energy in $\text{Er}^{3+}/\text{Yb}^{3+}$ co-doped glasses the red emission increases more than the green by means of the process described above. The presence of Ga_2O_3 also contributes to the relative enhancement of the red emission when compared to the green, as previously reported [34].

4. CONCLUSIONS

We have prepared and characterized $\text{Er}^{3+}/\text{Yb}^{3+}$ codoped lead bismuth gallium borate (GEY) glasses. Infrared spectra revealed the presence of various functional groups present in the glass system. With the help of optical absorption spectra and Judd-Ofelt theory, we have calculated the Ω_t ($t = 2, 4, 6$) intensity parameters, the oscillator strengths, branching ratios (β_r), and the radiative lifetimes of Er^{3+} doped glass. From the values of branching ratio it was found that the transition $^4\text{F}_{9/2} \rightarrow ^4\text{I}_{15/2}$ (660 nm) has the highest value of β_r among various transitions. This transition may therefore considered as a possible laser transition. The upconversion luminescence was recorded and investigated under the excitation of 980 nm laser diode. The intense red (660 nm) and weak green (525 and 545 nm) emissions are observed at room temperature. The red emission is more influenced than the green emissions and this is due to the fact that the probability of Er^{3+} ions relaxing non-radiatively from the $^4\text{F}_{11/2}$ level to the lower $^4\text{I}_{13/2}$ level is much higher than the probability of upconversion to the upper $^4\text{F}_{7/2}$ level as a result of the longer lifetime of the $^4\text{I}_{13/2}$ level compared to the lifetime of the $^4\text{I}_{11/2}$ level, which makes the non-radiative relaxation $^4\text{I}_{11/2} \rightarrow ^4\text{I}_{13/2}$ more easily to occur. The upconversion processes involved a sequential two-photon absorption for the green and red emissions. With increasing in the concentration of Er^{3+} upto 0.6 mol% (GE6Y2) the intensities of green (525 and 545 nm) increases slightly, while the red (660 nm) emission intensities increases very much more than that of green emissions. The presence of Ga_2O_3 also contributes and favors the red emission. The intense red upconversion luminescence of GE6Y2 glass can act as potential materials for developing upconversion optical devices.

REFERENCES

- [1] Collins, S. F., Baxter, G. W., and Wade, S. A., 1998, J. Appl. Phys., vol.84, pp. 4649.
- [2] Dai, S. X., Yang, J. H., and Xu, S. Q., 2003, Chin. Phys. Lett., vol.20, pp.130.

- [3] Zhang, L. Y., Yang, J.H., and Hu, L. L., 2003, *Chin. Phys. Lett.*, vol.20, pp.1344.
- [4] Kassab, L. R. P., Courrol, L. C., Seragioli, R., Wetter, N. U., Tatum, S. H., and Gomes, L., 2004, *J. Non. Cryst. Solids*, vol.348, pp.94.
- [5] Pisarski, W. A., Pisarska, J., Dominiak Dzik, G., and Ryba Romanowski, W., 2004, *J. Phys.: Condens. Matter*, vol.16, pp.6171.
- [6] Pisarski, W. A., Pisarska, J., Dominiak Dzik, G., Czka, M.M., and Ryba Romanowski, W., 2006, *J. Phys. Chem. Solids*, vol. 67, pp.2452.
- [7] Downing, E., Hesselink, L., Ralston, J., and Macfarlane, R. A., 1996, *three-color, solid-state, three dimensional display Science*, vol.273, pp.1185.
- [8] Branda, F., Costantini, A., Luciani, G., and Silvestri, B., 2004, *Phys. Chem. Glasses*, vol.45 pp.45.
- [9] Plucinski, K. J., Gruhn, W., and Wasylak Ebothe, J., 2003, *J. Opt. Mater.*, vol.22 pp.13.
- [10] Fiorenzo Vetrone, John-Christopher Boyer, John A. Capobianco, 2002, *Appl. Phys. Lett.*, vol.80, pp.1753.
- [11] Laporta, P., Longhi, S., Taccheo, S., et al., 1993, *Opt. Commun.*, vol.100, pp.311.
- [12] Qihua Nie, Longjun Lu, Tiefeng Xu, Shixun Dai, Xiang shen, Xiaowei Liang, Xudong Zhang and Xianghua Zhang, 2006, *J. Phy. and Chem. of Solids*, vol.67, 2345-2350.
- [13] Sands, R. H., 1995, *Phys. Rev.*, vol.99, pp.1222.
- [14] Davis, E. A., and Mott, N. F., 1970, *Phil. Mag.*, vol.22, pp. 903.
- [15] Judd, B. R., 1962, *Phys. Rev. Vol.127*, pp.750.
- [16] Ofelt, G. S., 1962, *J.Chem. Phys.*, vol.37, pp.511.
- [17] De la Rosa-Cruz, E., Kumar, G. A., Diaz-Torres, L. A., Martinez, A., and Barbosa-Garcia, O., 2001, *Opt.Mater.*, vol.18, pp.321.
- [18] Choi, J. H., Margaryan, A., and Shi, F. G., 2005, *J. Lumin.*, vol.114, pp.167.
- [19] Krupke, W. F., 1966, *Phys. Rev.*, vol.145, pp.325.
- [20] Carnall, W. T., Fields, P. R., and Wybourne, B. G., 1965, *J. Chem. Phys.*, vol.42, pp.3797.
- [21] Weber, M., 1967, *J. Phys. Rev.*, vol.157, pp.262.
- [22] Mehta, V., Aka, G., Dawar, A. L., and Mansingh, A., 1999, *Opt. Mater.*, vol.12, pp.53.
- [23] Bomfim, F. A., Martinelli, J. R., Kassab, L. R. P., Wetter, N. U., and Neto, J. J., 2009, *J. Non-Cryst. Solids*, vol.354 pp.256-260.
- [24] Sharma, Y. K., Surana, S. S. L., and Singh, R. K., 2008, *Indian Journal of Pure and Applied Physics*, vol.46, pp.239-244.
- [25] Veerabhadra Rao, A., Laxmikanth, C., Appa Rao, B., and Veeraiah, N., 2006, *J. Phys. Chem. Solids*, vol.67, pp.2263.
- [26] De. Andrade, J. S., Pinheiro, A. G., Vasconcelos, I. F., Sasaki, J. M., Paiva, J. A. C. D. E., Valente, M. A., and Sombra, A .S. B., 1999, *J. Phys. Condens. Matter*, vol.11, pp.4415.

- [27] Hung, W. H., Ray, C. S., and Ray, D. E., 1994, *J. Am. Ceram. Soc.*, vol.77, pp.1071.
- [28] Yeh, D. C., Sibley, W. A., and Suscavage, M., 1987, *J. Appl. Phys.*, vol.62, pp.266.
- [29] Huang, L. H., Liu, X. R., Xu, W., Chen, B. J., and Lin, J. L., 2001, *J. Appl. Phys.*, vol.90, pp.5550–5553.
- [30] Lin, H., Meredith, G., Jiang, S., Peng, X., Luo, T., Peyghambarian, N., and Pun, E.Y.B., 2003, *J. Appl. Phys.*, vol.93, pp.186–191.
- [31] Adam, J. L., 2001, *J. Fluorine Chem.*, vol.107, pp.265.
- [32] Cantelar, E., and Cussó, F., 2003, *J. Lumin.*, vol.102, pp.525.
- [33] Yamauchi, H., and Ohishi, Y., 2005, *Opt. Mater.*, vol.27, pp.679.
- [34] Nie, Q., Jiang, C., Wang, X., Xu, T., and Li, H., 2007, *Spectrochim. Acta Part A*, vol.66, pp.278.
- [35] Shiqing Xu, Guonian Wang, Shixun Dai, Junjie Zhang, Lili Hu, and Zhonghong Jiang, 2004, *J. solid state chem.*, vol.177, pp.3127-3130.

